J. Am. Soc. Mass Spectrom. (2016) 27:394–401
DOI: 10.1007/s13361-015-1296-6

RESEARCH ARTICLE

Competitive Deprotonation and Superoxide [$O_2^{-\bullet}$] Radical-Anion Adduct Formation Reactions of Carboxamides under Negative-Ion Atmospheric-Pressure Helium-Plasma Ionization (HePI) Conditions

Isra Hassan, Spencer Pinto, Carl Weisbecker, Athula B. Attygalle

Center for Mass Spectrometry, Department of Chemistry, Chemical Biology, and Biomedical Engineering, Stevens Institute of Technology, Hoboken, NJ 07030, USA

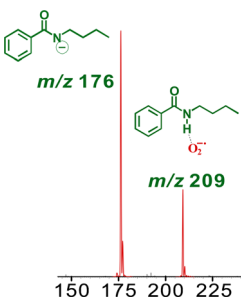

Abstract. Carboxamides bearing an N–H functionality are known to undergo deprotonation under negative-ion-generating mass spectrometric conditions. Herein, we report that N–H bearing carboxamides with acidities lower than that of the hydroperoxyl radical (HO-O$^\bullet$) preferentially form superoxide radical-anion ($O_2^{-\bullet}$) adducts, rather than deprotonate, when they are exposed to the glow discharge of a helium-plasma ionization source. For example, the spectra of *N*-alkylacetamides show peaks for superoxide radical-anion ($O_2^{-\bullet}$) adducts. Conversely, more acidic amides, such as *N*-alkyltrifluoroacetamides, preferentially undergo deprotonation under similar experimental conditions. Upon collisional activation, the $O_2^{-\bullet}$ adducts of *N*-alkylacetamides either lose the neutral amide or the hydroperoxyl radical (HO-O$^\bullet$) to generate the superoxide radical-anion (*m/z* 32) or the deprotonated amide [*m/z* (M – H)$^-$], respectively. For somewhat acidic carboxamides, the association between the two entities is weak. Thus, upon mildest collisional activation, the adduct dissociates to eject the superoxide anion. Superoxide-adduct formation results are useful for structure determination purposes because carboxamides devoid of a N–H functionality undergo neither deprotonation nor adduct formation under HePI conditions.

Keywords: Helium-plasma ionization (HePI), Carboxamides, Superoxide radical anion, Adducts

Received: 30 May 2015/Revised: 15 October 2015/Accepted: 16 October 2015/Published Online: 6 November 2015

Introduction

Certain gaseous molecules are known to undergo anion attachment under negative-ion-generating atmospheric pressure or vacuum chemical ionization (APCI) conditions [1–4]. One of the gaseous anions found in the plasma of discharge ion sources under negative-ion-generating conditions is the superoxide radical-anion, $O_2^{-\bullet}$ [5–9]. Sometimes, $O_2^{-\bullet}$ has been generated under pulsed positive- and negative-ion chemical ionization conditions, using a mixture of hydrogen and oxygen as the reagent gas [10]. The attachment of this superoxide radical-anion to several gaseous molecules has been documented. For example, the formation of adducts with $O_2^{-\bullet}$ has been noted for alcohols [6, 11], ketones [12], phenols [13], tetrachlorodioxins [14], polyethers [15], phthalates [16, 17], and some tricothecenes [7]. Recently, Cody and Dane reported the formation of $O_2^{-\bullet}$ adducts of linear aliphatic hydrocarbons, alcohols, and esters under direct analysis in real time (DART) conditions [18]. To the best of our knowledge, such an adduct formation has not been reported for amides. Moreover, the molecular properties that determine the specificity of $O_2^{-\bullet}$ adduct formation, or the details of the mechanisms involved in the adduct formation, are poorly understood. Under negative-ion-generating conditions, polyaromatic and halogenated compounds undergo resonance electron capture because of the availability of unoccupied low-energy molecular orbitals (LUMO) [19]. However, this LUMO-orbital model cannot rationalize the $O_2^{-\bullet}$ adduct formation from alkanes and alcohols. At least for

Electronic supplementary material The online version of this article (doi:10.1007/s13361-015-1296-6) contains supplementary material, which is available to authorized users.

Correspondence to: Athula Attygalle; *e-mail:* aattygal@stevens.edu

large alkanes, it has been postulated that their high polarizability affords longer lifetimes of adducts formed due to collisional cooling [18]. However, it has been recognized that this model cannot be applied to the formation of alcohol adducts [18]. Thus, a hydrogen bonding model has been proposed as a more suitable explanation [18].

Although $O_2^{-\bullet}$ is known to be an efficient proton-abstracting agent because of its basicity [gas-phase acidity of HO–O$^\bullet$ = 346.7 kcal/mol {$\Delta G_{reaction}$ of HO–O$^\bullet$ (gas) ➔ O=O $^{-\bullet}$ (gas) + H^+ (gas)}; proton affinity (ΔH) of $O_2^{-\bullet}$ = 353.0 ± 0.7 kcal/mol) [5, 20–22], our explorations with helium-plasma ionization (HePI) of small molecules have shown that certain carboxamides also undergo facile ionization by forming $O_2^{-\bullet}$ adducts. Thus, the basicity of the superoxide radical-anion should be considered as moderate (it is more basic than the chloride or nitrite ions but less basic than the fluoride or anilide ions) [23]. For mass-spectrometric monitoring of carboxamides, the positive-ion-generating mode is generally preferred because the carboxamide moiety readily undergoes protonation under electrospray ionization conditions. However, it has been demonstrated that carboxamides synthesized from primary amines can be deprotonated under negative-ion electrospray [24] and OH^- chemical-ionization conditions [25–27]. Herein, we report that under HePI conditions, carboxamides undergo $O_2^{-\bullet}$ adduct formation and/or deprotonation, and we discuss the significance of the chemical nature of the N–H functionality for the $O_2^{-\bullet}$ attachment.

Experimental

Reagents

All reagents and solvents were purchased from Aldrich Chemical Co. (St. Louis, MO, USA) and used as obtained.

Derivatization

For the preparation of the acetyl derivatives, each amine was treated with a mixture (1 mL) of acetic anhydride (95%) and pyridine (5%). After 5 min, the reaction mixture was acidified with 1 M HCl (0.75 mL), and extracted into dichloromethane (1 mL). The extracts were then dried with a stream of N_2 to obtain the products as solids or oily residues. Similarly, trifluoroacetamides were synthesized by adding trifluoroacetic anhydride (1 mL) to each amine (0.5 mL). Benzamides were synthesized by adding benzoyl chloride (1 mL) to each amine (0.5 mL) [28].

Gas Chromatography–Mass Spectrometry (GC-MS)

Samples (1.0 mg/mL in dichloromethane) were introduced by split injection to a Hewlett Packard 5890 Series II gas chromatograph equipped with a 30 m × 0.25 mm capillary column coated with a 0.25-µm film of XTI-5 (5% diphenyl/95% dimethyl polysiloxane; Restek, Bellefonte, PA, USA), connected to an HP 5970 quadrupole mass spectrometer. The oven temperature was held at 40°C for 4.0 min and increased (8°C/min) to a final temperature of 250°C. The temperature was then held at 250°C for 10 min. Electron ionization (EI) mass spectra (70 eV) were recorded from all synthetic samples and compared with the previously reported EI spectra [29], and EI spectra in the NIST/EPA/NIH mass spectral database [30].

N-(octan-2-yl)benzamide: EI *m/z* (%), 233($M^{+\bullet}$, 89), 149(7), 148(23), 122(9), 106(7), 105(100), 77(3), 55(3), 51(8), 44(3), 43(6), 42(4), 41(11).
N-benzylacetamide: EI-MS *m/z* (%), 149($M^{+\bullet}$, 74), 106(100), 104(9), 92(4), 91(38), 89(5), 79(19), 78(10), 77(26), 76(3), 74(3), 65(13), 63(6), 52(6), 51(21), 50(10), 43(46), 42(5), 41(3), 39(10).
N-dodecylbenzamide: EI-MS *m/z* (%), 289($M^{+\bullet}$, 55), 135(26), 134(24), 105(100), 77(34), 43(18), 41(15).
N-(4-bromophenyl)acetamide EI-MS *m/z* (%), 214($M^{+\bullet}$, 6), 173(43), 171(48), 92(41), 65(35), 64(19), 63(28), 43(100).
N-(4-fluorophenyl)acetamide: EI-MS *m/z* (%), 153($M^{+\bullet}$, 13), 112(7), 111(100), 84(14), 83(13), 63(3),57(9), 43(30).
N-(2-chlorophenyl)acetamide: EI-MS *m/z* (%), 170($M^{+\bullet}$, 10), 134(29), 129(31), 127(100), 99(8), 92(9), 91(5), 90(4), 75(4), 73(5), 65(8), 64(7), 63(10), 52(3), 43(41), 39(6), 38(5).
N-butylbenzamide: EI-MS *m/z* (%), 177($M^{+\bullet}$, 2), 135(9), 134(10), 106(7), 78(4), 77(48), 51(19), 50(6), 41(7), 39(5).
N-pentylbenzamide: EI-MS *m/z* (%), 191($M^{+\bullet}$, 11), 135(7), 134(11), 106(7), 105(100), 77(52), 51(17), 50(5), 41(9), 39(5).
N-phenethylbenzamide: EI-MS *m/z* (%), 225($M^{+\bullet}$, 14), 134(5), 106(7), 105(100), 104(35), 91(12), 78(6), 77(53), 65(9), 51(20), 50(6), 39(6).
N-*p*-tolylacetamide: EI-MS *m/z* (%), 149($M^{+\bullet}$, 42), 107(91), 106(100), 91(5), 79(12), 78(12), 77(30), 63(5), 51(14), 43(29), 37(1).
N-(2-(2-aminoethylamino)ethyl)acetamide: EI-MS *m/z* (%), 145($M^{+\bullet}$, 8), 128(2), 115(55), 110(1), 99(12), 86(100), 73(15), 56(11), 43(93).

Helium-Plasma Ionization (HePI) Mass Spectrometry

For the generation of the HePI plasma, a stream of high purity helium (99.999%, Airgas, Radnor, PA, USA) was passed through a metal capillary held at a high voltage [31]. The metal capillary tip was set about 10 mm from the mass analyzer entrance-cone orifice of a Waters Micromass Quattro Ultima mass spectrometer (Waters Corp., Manchester, UK). Typically, the helium flow rate was maintained at 30 mL/min, and the capillary voltage was set at 2.5–3.5 kV (adjusted to obtain the optimal ion flux).

The source temperature was held at 150°C. The cone voltage was typically set at 10 V, and hexapole I transfer lens was held at 20–30 V. For MS/MS experiments, the pressure of the argon in the collision cell was maintained at 2.5×10^{-5} mbar. The heater of the desolvation gas line was used to increase the temperature of the nitrogen desolvation gas to facilitate the thermal desorption of analytes. Typically, the "desolvation"

temperature was set between 250 and 400°C. Samples were deposited on a glass slide and placed in the open source about 1 cm from the capillary orifice.

Hydrogen-Deuterium Exchange Experiments

The sample was dissolved in dry acetonitrile and mixed with a drop of D_2O. The solvent was then evaporated with a stream of nitrogen gas to obtain a solid residue, which was placed in the ion source for mass spectrometric analysis.

Computational Methods

The Gaussian 09 program, [32] using the B3LYP [33] method and 6-311G ++ (2d,2p) basis-set for all atoms, was used to perform quantum mechanics (QM) calculations. All molecules were fully optimized without any constraints. Frequency analysis was done at the same level to confirm that the optimized structures correspond to the minimum-energy states on the respective potential energy surfaces. Computations were also conducted using the CAM-B3LYP functional method and 6-31G+(d,p) basis-set to account for the dispersion corrections because the B3LYP functional may not treat the long range ion–dipole interactions effectively.

Calculation of Gibbs Free Energy

Gibbs free energy values were calculated at a temperature of 298.15 K and a pressure of 1.0 atm. However, calculated zero-point energies and Gibbs free energy values were not adjusted using an empirical scaling factor.

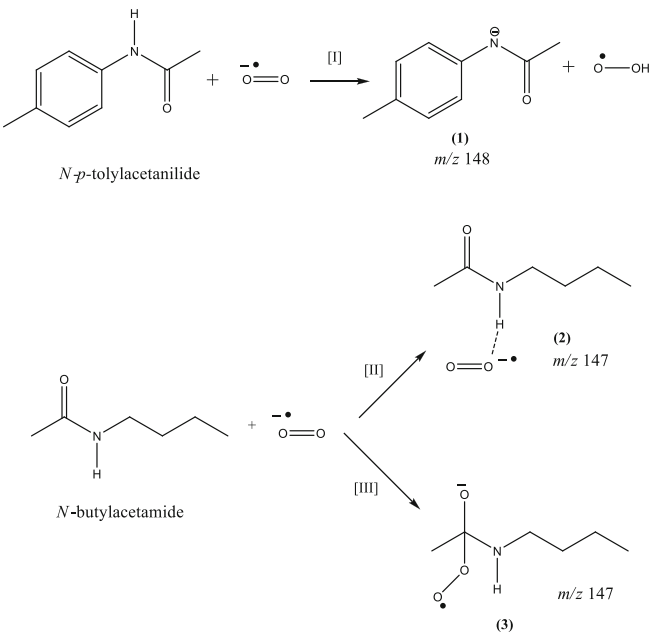

Scheme 1. Proposed ionization pathways of *N*-*p*-tolylacetamide and *N*-butylacetamide under HePI conditions

Calculation of Gas Phase Acidity

The gas-phase acidity was computed as the Gibbs free energy (ΔG) of the reaction (values obtained from Gaussian 09 output files) when the neutral amide is deprotonated ($AH \rightarrow A^- + H^+$). According to Burk et al., rational predictions of gas phase acidities can be obtained at the B3LYP/6-311G++ level of theory [34].

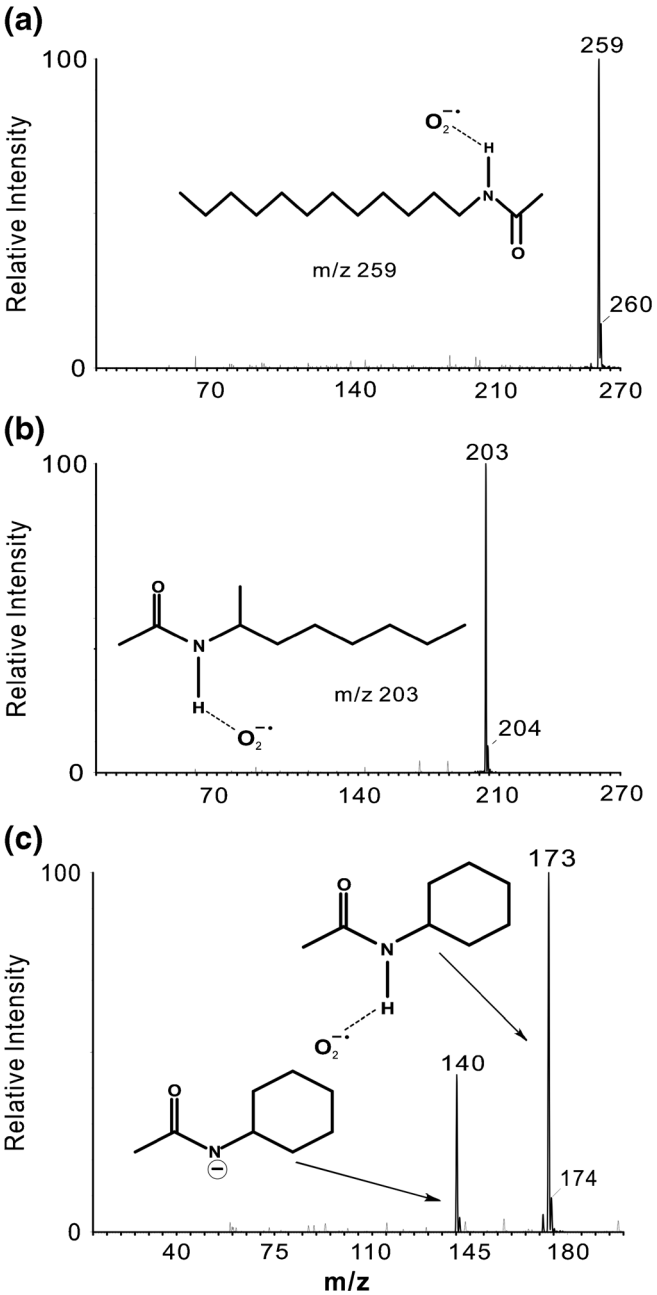

Figure 1. HePI mass spectra recorded under negative-ion generating conditions from *N*-dodecylacetamide **(a)**, *N*-(octan-2-yl)acetamide **(b)**, and *N*-cyclohexylacetamide **(c)** (capillary voltage –3.7 kV, a cone voltage of 10 V; hexapole 1 voltage 11.6 V; source temperature 150°C; desolvation gas temperature 350°C)

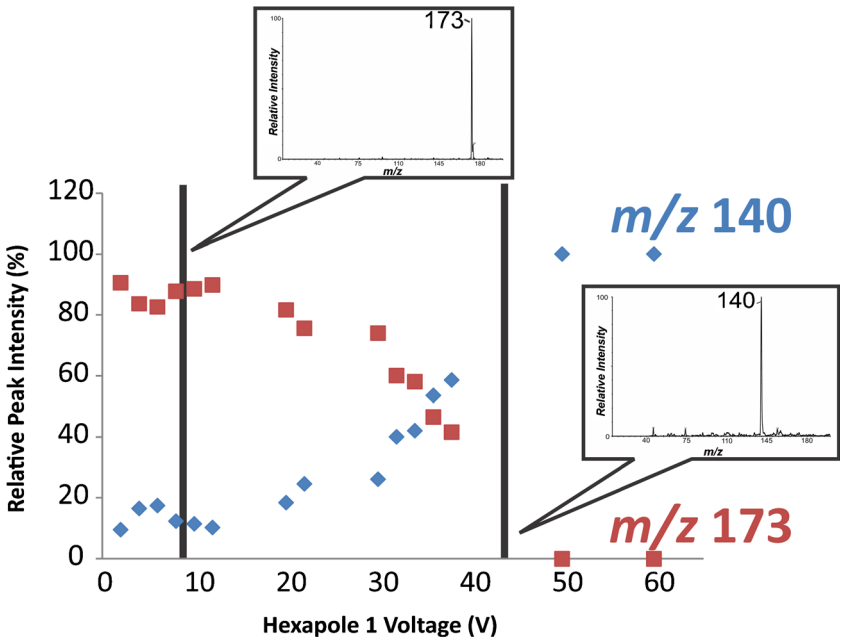

Figure 2. Plot of percentage relative intensities of the *m/z* 173 (-♦-), and 140 (-■-) peaks derived from spectra recorded for *N*-cyclohexylacetamide at different hexapole I voltage settings (cone voltage 10 V; capillary voltage –3.3 kV; source temperature 150°C; desolvation gas temperature 350°C). The two insets show typical spectra observed at hexapole I voltages of 8 and 42 V, respectively

Results and Discussion

Under negative-ion-generating helium-plasma ionization (HePI) mass spectrometric conditions, most carboxamides undergo deprotonation. For example, the spectrum recorded from *N*-*p*-tolylacetamide showed an intense peak at *m/z* 148 for the $(M - H)^-$ ion (Supplementary Figure 1; Scheme 1, Path I). However, to our surprise, spectra recorded from many other amides failed to produce significant peaks for the deprotonated molecules. For example, the spectrum recorded from *N*-dodecylacetamide did not generate a visible peak at *m/z* 226 (Figure 1a). Instead, an intense peak was observed at *m/z* 259. Evidently, the peak at *m/z* 259 represented an $O_2^{-\bullet}$ adduct of *N*-dodecylacetamide. Analogously, in the HePI spectrum of *N*-(octan-2-yl)acetamide, a peak at *m/z* 203 was observed, which was attributed to the $O_2^{-\bullet}$ adduct of the parent amide (Figure 1b). On the other hand, the spectrum recorded from *N*-cyclohexylacetamide showed peaks for both species (deprotonated molecule and $O_2^{-\bullet}$ adduct at *m/z* 140 and 173, respectively; Figure 1c).

Further experimentation showed that the intensity of the $O_2^{-\bullet}$ adduct peak is highly dependent on the ionization source conditions. Evidently, low cone voltages (the voltage bias between the entrance orifice and the skimmer of the low-vacuum source region) favors greater adduct formation. A similar effect has been noted by Cody and Dane under direct analysis in real time (DART) conditions [18]. For *N*-cyclohexylacetamide, a cone setting of about 10 V provided the optimal adduct formation conditions (Figure 1c). In fact, the changes to the voltage bias between the two ends of the first hexapole transfer lens of the Quattro mass spectrometer had a more pronounced effect on the abundance of the adduct. For example, the intensity of the $O_2^{-\bullet}$ adduct peak from *N*-cyclohexylacetamide (*m/z* 173) decreased rapidly at potential differences higher than 10 V, whereas that for the deprotonated molecule (*m/z* 140) increased (Figure 2). Although the trendlines were not smooth, the plots clearly demonstrated the general tendencies of intensity changes.

Furthermore, the adduct formation is also influenced by the temperature of the ion source. As the source-block temperature

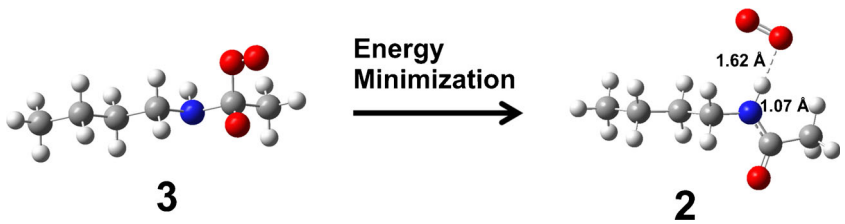

Figure 3. Energy minimization of the superoxide anion adduct of *N*-butylacetamide (color scheme: carbon, dark gray, hydrogen, light gray, oxygen, red, and nitrogen, blue)

was increased, the relative intensity of the superoxide radical-anion-adduct peak observed for *N*-cyclohexylacetamide (*m/z* 173) gradually decreased, whereas that of the deprotonated amide (*m/z* 140) did not show any significant changes (Supplementary Figure 2). This observation suggests that adduct formation is not favored for kinetically excited molecules.

The structure of the $O_2^{-\bullet}$ adducts and the mechanism of their formation have not been elucidated in previous investigations [18]. In solution chemistry, the superoxide radical-anion is known to attack the carbonyl group as a nucleophile [35]. A similar mechanism has been proposed for the adduct formation with phenyl benzoates [16]. Because $O_2^{-\bullet}$ is known to form conjugates even with non-carbonyl compounds, such as hydrocarbons and alcohols, we presumed the mechanism of adduct formation with carboxamides to be different [18]. We postulated that the addition to amides takes place via the N–H bond (Scheme 1, Path II) and not via the carbonyl group as proposed for solution-based methods, or gas-phase methods for esters [18] (Scheme 1, Path III).

To scrutinize our postulate, we conducted computational energy minimizations on several hypothetical structures of the $O_2^{-\bullet}$ adduct formed from *N*-butylacetamide (Scheme 1), using two computational protocols: B3LYP method with a 6-311G ++ (2d,2p) basis-set and the CAM-B3LYP functional method with a 6-31G+(d,p) basis-set. However, we could not find an energy-minimized configuration for a structure in which the superoxide radical-anion has been added to the carbon atom of the carbonyl group (Structure 3, Scheme 1). Because the B3LYP functional does not treat the long range ion–dipole interactions effectively, we employed also the CAM-B3LYP functional method, which is considered to account for the dispersion corrections. In fact, during the process of energy minimization by both methods, the covalently bonded adduct (Structure 3) converged to produce Structure 2, in which the oxygen of the superoxide radical-anion is noncovalently bonded to the amide hydrogen. In other words, computations supported the supposition that Structure 2 is the preferable structure of the adduct that exists in the gas phase (Figure 3, and Supplementary Figure 6). However, we note that for benzenedicarboxylate esters, the $O_2^{-\bullet}$ addition reaction takes place at the carbonyl carbon [16].

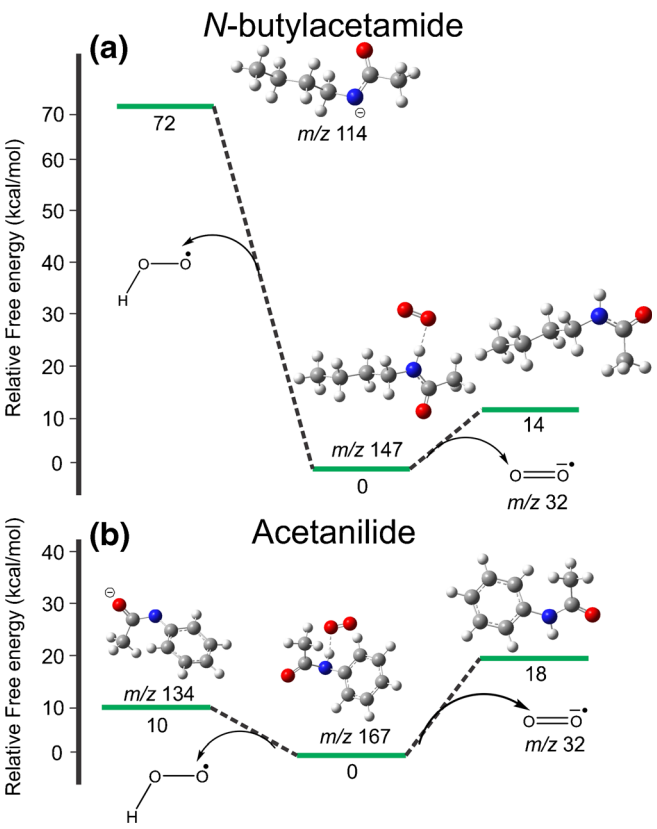

Figure 4. Schematic illustration of relative Gibbs free energies (in kcal/mol) of the product ions produced as a result of the fragmentation of the superoxide radical anion adducts of *N*-butylacetamide **(a)**, and acetanilide **(b)**

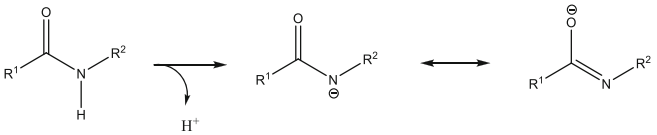

Scheme 2. Deprotonation of a secondary amide

To establish diagnostically useful generalizations on $O_2^{-\bullet}$ adduct formation, we recorded spectra of many acetylated amines. The results suggest that only the derivatives generated from primary aliphatic amines form $O_2^{-\bullet}$ adducts (Supplementary Table 1).

In contrast, the spectra recorded from aniline derivatives or *N*-trifluoroacetamides failed to show peaks for $O_2^{-\bullet}$ adducts (Supplementary Table 2). Computational calculations support these results and show that it is much more favorable for $O_2^{-\bullet}$ to abstract the proton of an aromatic amide ($\Delta G = 10$ kcal mol^{-1}) as opposed to abstracting the proton of an aliphatic amide ($\Delta G = 72$ kcal mol^{-1}) (Figure 4). However, compounds such as benzamide and *N*-phenylethylbenzamide, even though they are aromatic, do undergo $O_2^{-\bullet}$ adduct formation (Supplementary Figure 3). Moreover, tertiary amides derived from secondary amines failed to form $O_2^{-\bullet}$ adducts because they do not bear an N–H bond.

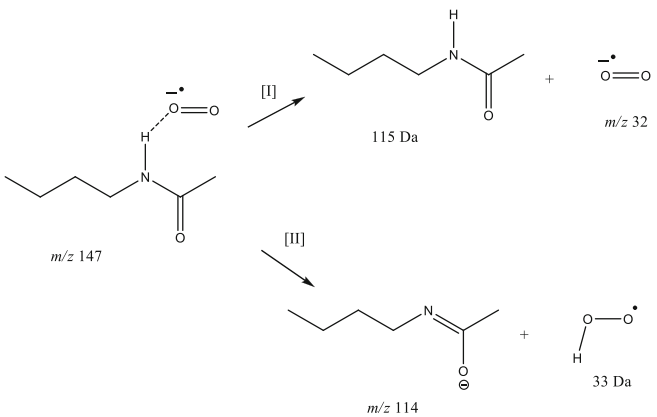

Scheme 3. Proposed fragmentation pathways of the $O_2^{-\bullet}$ adduct of *N*-butylacetamide

To deprotonate a carboxamide, gaseous superoxide radical anions present in the HePI source should act as a base. Upon abstracting a proton from the amide, it forms a hydroperoxyl radical (H-O-O$^{\bullet}$) as a by-product. The gas-phase acidity of the hydroperoxyl radical is known to be 346.7 ± 0.8 kcal mol^{-1} [20–22]. We computed the gas-phase acidity of the hydroperoxyl radical by the density functional theory method B3LYP with a 6-311G++ basis set using Gaussian 09 program. The value obtained, 346.7 kcal/mol, was in excellent accord with the literature value 346.7 kcal/mol given in NIST webbook [22], which indicated that the values computed for other carboxamides are credible. When the analyte amide is less acidic (larger ΔG_{acid} value) than that of the hydroperoxyl radical, then the $O_2^{-\bullet}$ attachment appears to be favored. In contrast, when the amide to be ionized is more acidic than the hydroperoxyl radical (e.g., *N*-butyl-2,2,2-trifluoroacetamide), the deprotonation process is favored (Supplementary Table 3).

Aliphatic and aromatic carboxamides in solution are generally regarded as pH-neutral compounds. However, amides derived from primary amines exhibit a certain degree of acidity because the removal of a proton from the N–H functionality generates a charge-delocalized anion (Scheme 2). From the data available, it appears that more acidic amides generally undergo deprotonation (Supplementary Table 2), whereas less acidic amides undergo adduct formation when they encounter $O_2^{-\bullet}$ ions (Supplementary Table 1). Analogously, the strong electron-withdrawing properties of the trifluoromethyl group render trifluoroacetamides significantly acidic (R^1 = CF_3; Scheme 2), to suppress the formation of $O_2^{-\bullet}$ adducts from this group of compounds (Supplementary Table 2). The computed value for the gas-phase acidity of the trifluoroacetamide listed in Supplementary Table 3 supports these observations.

Upon collisional activation, the $O_2^{-\bullet}$ adducts generated from amides undergo fragmentation by two different pathways (Scheme 3). For example, the CID mass spectrum recorded from the $O_2^{-\bullet}$ adduct of *N*-cyclohexylacetamide (*m/z* 173) showed a significant peak at *m/z* 32 for the superoxide radical-anion because of the ejection of *N*-cyclohexylacetamide as a neutral species but a much smaller peak at *m/z* 140 for the loss of H-O-O$^{\bullet}$ radical (Figure 5a). Product-ion mass spectra support that the $O_2^{-\bullet}$ adduct of *N*-butylacetamide (*m/z* 147) fragments in a similar manner (Supplementary Table 1). Computations confirmed that the $O_2^{-\bullet}$ adduct of *N*-butylacetamide requires much more energy (72 kcal/mol) to lose an H-O-O$^{\bullet}$ radical as opposed to a neutral amide (14 kcal/mol) (Figure 4). Further computational evaluations showed that the bond between the amide hydrogen and the $O_2^{-\bullet}$ oxygen is longer (1.62 Å) than the N–H bond (1.07 Å) (Figure 3), indicating that the O–H bond is weaker and more likely to break upon collisional activation. In other words, for somewhat acidic compounds, even if an adduct is formed, the noncovalent association between the two entities is weak. Thus, upon mildest collisional activation, the association breaks to eject the superoxide anion. For example, the association between the superoxide anion and *N*-cyclohexylacetamide or *N*-phenylethylacetamide (the computed gas-phase acidities for which are 358.0 and 354.3 kcal/mol; Supplementary Table 3) is considered weak, and upon collisional activation they break to generate $O_2^{-\bullet}$ (Figure 5a and

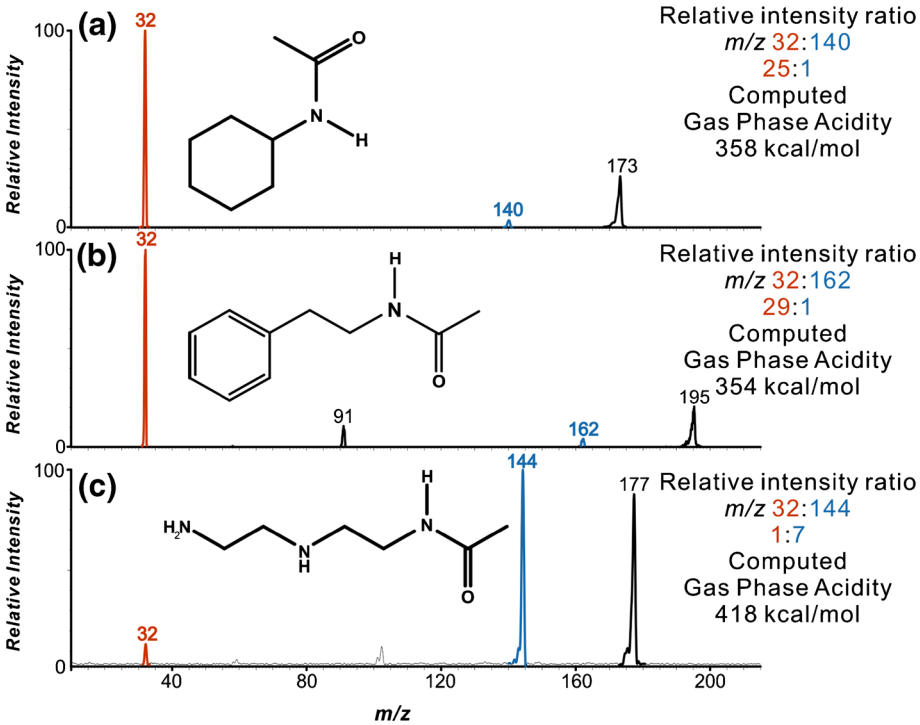

Figure 5. Product-ion spectra recorded from *m/z* 173, 195, and 177 ions generated from *N*-cyclohexylacetamide **(a)**, *N*-phenylethylacetamide **(b)**, and *N*-(2-(2-aminoethylamino)acetamide **(c)**, respectively (capillary voltage of –2.9 kV; cone voltage of 10 V; hexapole I transfer lens voltage 10 V; collision energy 20 eV; source temperature 150°C, desolvation gas temperature 250°C)

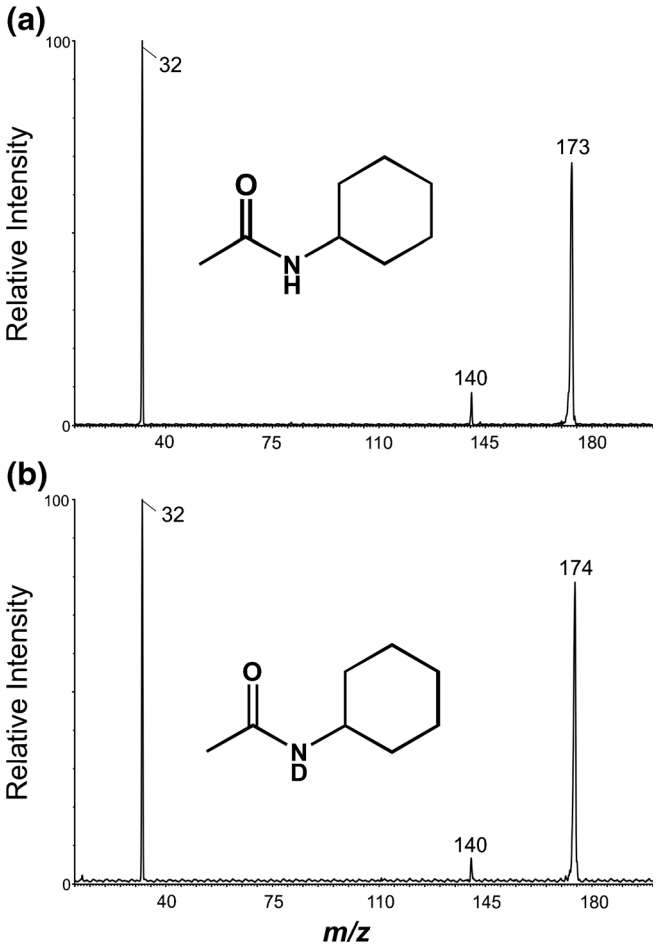

Figure 6. Product-ion mass spectrum recorded from *m/z* 173 ion generated from *N*-cyclohexylacetamide **(a)**, and that of *m/z* 174 ion **(b)**, derived from a D/H-exchanged sample (capillary voltage –3.80 kV; cone voltage of 10 V; hexapole transfer lens voltage 15 V; source temperature 148°C, desolvation temperature of 400°C)

b). In contrast, the *m/z* 177 adduct ion generated from the less acidic *N*-(2-(2-aminoethylamino)-ethyl) acetamide (computed gas phase acidity 418.7 kcal/mol; Supplementary Table 3) ejected an H-O-O$^{\bullet}$ radical to form an *m/z* 144 ion for the deprotonated amide (Figure 5c).

To confirm that the hydrogen atom at the N–H bond of the amide participates in the radical loss of H-O-O$^{\bullet}$, a hydrogen–deuterium exchange experiment was conducted using *N*-cyclohexylacetamide as the test compound. The HePI spectrum recorded from a deuterium-exchanged sample showed an additional peak at *m/z* 174 to indicate that the labile amide hydrogen atom had been replaced by a deuteron (Supplementary Figure 4). The product-ion spectrum recorded upon CID activation of the mass-isolated *m/z* 174 showed a peak at *m/z* 140 (Figure 6). The peak at *m/z* 140, which represents the loss of a 34-Da D-O-O$^{\bullet}$ radical, supports the fragmentation mechanism presented in Scheme 3. The proposed mechanism was further supported by the kinetic isotope effect witnessed from the deuterium-labeled sample. The fragmentation of the *m/z* 173 and 174 ions, generated from the unlabeled and labeled samples, respectively, produced a peak at *m/z* 140 in both cases, but with two different relative intensities (Figure 6). The ratio of the relative intensities of the *m/z* 173:140 peaks was determined to be 8.05 (Figure 6a); this value differs from the ratio of the relative intensities of *m/z* 174:140, which is 11.7 (Figure 6b). This result demonstrated that the amide hydrogen directly participates in the H-O-O$^{\bullet}$ radical loss.

Aliphatic amides are found in many everyday products, one of which is chewing gum. WS-23, an amide found in chewing gum (specifically 5 peppermint cobalt gum), serves as a flavoring agent. Supplementary Figure 5 shows that WS-23 forms a superoxide radical anion adduct.

Conclusions

From the observed results on carboxamide spectra under HePI conditions, we make the following diagnostically useful conclusions: (1) Only certain carboxamides generate $O_2^{-\bullet}$ adducts under HePI conditions. (2) N–H bearing carboxamides of low acidity (derived from primary aliphatic amines) form $O_2^{-\bullet}$ adducts. (3) Relatively acidic carboxamides, such as trifluoroacetamides and anilides do not form $O_2^{-\bullet}$ adducts. (4) Relatively acidic carboxamides, such as trifluoroacetamides and anilides undergo deprotonation to produce an $(M - H)^-$ ion. (5) Carboxamides that do not bear a N–H functionality neither form $O_2^{-\bullet}$ adducts nor produce deprotonated molecules.

Moreover, our results suggest that the gas-phase acidity owing to the N–H functionality (when present) is one of the criteria that determine the degree of adduct formation with the superoxide radical-anion. More acidic substrates are deprotonated by $O_2^{-\bullet}$ acting as a base. In contrast, weaker acids undergo adduct formation. Presumably, our hypothetical model could be used to rationalize the formation of superoxide radical-anion adducts from other compounds such as alcohols and hydrocarbons as well.

Acknowledgments

The authors thank Bristol-Myers Squibb Pharmaceutical Company (New Brunswick, NJ) for the donation of the Waters Quattro mass spectrometer.

References

1. Zencak, Z., Oehme, M.: Chloride-enhanced atmospheric pressure chemical ionization mass spectrometry of polychlorinated *n*-alkanes. Rapid Commun. Mass Spectrom. **18**, 2235–2240 (2004)
2. Tannenbaum, H.P., Roberts, J.D., Dougherty, R.C.: Negative chemical ionization mass spectrometry-chloride attachment spectra. Anal. Chem. **47**, 49–54 (1975)
3. Dougherty, R.C., Roberts, J.D., Biros, F.J.: Positive and negative chemical ionization mass spectra of some aromatic chlorinated pesticides. Anal. Chem. **47**, 54–59 (1975)
4. Morgan, R.P., Gilchrist, C.A., Jennings, K.R., Gregor, I.K.: Selective chemical ionization using chloride ions. Int. J. Mass Spectrom. Ion. Phys. **46**, 309–312 (1983)
5. Dzidic, I., Carroll, D.I., Stillwell, R.N., Horning, E.C.: Gas phase reactions. Ionization by proton transfer to superoxide anions. J. Am. Chem. Soc. **96**, 5258–5259 (1974)

6. Hunt, D.F., McEwen, C.N., Harvey, T.M.: Positive and negative chemical ionization mass spectrometry using a Townsend discharge ion source. Anal. Chem. **47**, 1730–1734 (1975)
7. Miles, W.F., Gurprasad, N.P.: Oxygen negative chemical ionization mass spectrometry of trichothecenes. Biomed. Mass Spectrom. **12**, 652–658 (1985)
8. Miles, W.F., Gurprasad, N.P., Malis, G.P.: Isomer-specific determination of hexachlorodibenzo-*p*-dioxins by oxygen negative chemical ionization mass spectrometry, gas chromatography, and high-pressure liquid chromatography. Anal. Chem. **57**, 1133–1138 (1985)
9. Moruzzi, J.L., Phelps, A.V.: Survey of negative-ion–molecule reactions in O_2, CO_2, H_2O, CO, and mixtures of these gases at high pressures. J. Chem. Phys. **45**, 4617–4627 (1966)
10. Hunt, D.F., Stafford, G.C., Crow, F.W., Russel, J.W.: Pulsed positive and negative ion chemical ionization mass spectrometry. Anal. Chem. **48**, 2098–2105 (1976)
11. Futrell, J.H., Tiernan, T.O.: In: Franklin, J.L. (ed.) Ion-Molecule Reactions. Plenum, New York (1972)
12. McDonald, R.N., Chowdhury, A.K.: Gas-phase ion-molecule reactions of dioxygen anion radical ($O_2^{-\bullet}$). J. Am. Chem. Soc. **107**, 4123–4128 (1985)
13. Zhou, Q., Hua, L., Wang, C., Li, E., Li, H.: Improved analytical performance of negative ^{63}Ni ion mobility spectrometry for on-line measurement of propofol using dichloromethane as dopant. J. Am. Soc. Mass Spectrom. **26**, 190–193 (2015)
14. Hunt, D.F., Harvey, T.M., Russell, J.W.: Oxygen as a reagent gas for the analysis of 2,3,7,8-tetrachlorodibenzo-*p*-dioxin by negative ion chemical ionization mass spectrometry. J. Chem. Soc. Chem. Commun. **5**, 151–152 (1975)
15. Available at: http://www.jeolusa.com/DesktopModules/Bring2mind/DMX/Download.aspx?EntryId=384&Command=Core_Download&PortalId=2&TabId=337. Accessed August 6, 2015
16. Stemmler, E.A., Diener, J.L., Swift, J.A.: Gas-phase reactions of $O_2^{-\bullet}$ with alkyl and aryl esters of benzenedicarboxylic acids. J. Am. Soc. Mass Spectrom. **5**, 990–1000 (1994)
17. Lépine, F., Boismenu, D., Milot, S., Orval, A., Mame, O.A.: Collision of molecular anions of benzenedicarboxylic esters with oxygen in a triple quadrupole mass spectrometer. J. Am. Soc. Mass Spectrom. **10**, 1248–1252 (1999)
18. Cody, R.B., Dane, A.J.: Soft ionization of saturated hydrocarbons, alcohols and nonpolar compounds by negative-ion direct analysis in real-time mass spectrometry. J. Am. Soc. Mass Spectrom. **24**, 329–334 (2013)
19. Pshenichnyuka, S.A., Kukhtob, A.V., Kukhtob, I.N., Asfandiarov, N.L.: Resonance capture of electrons by electroactive organic molecules. Russ. J. Phys. Chem. B **4**, 1014–1027 (2010)
20. Travers, M.J., Cowles, D.C., Ellison, G.B.: Reinvestigation of the electron affinities of O_2 and NO. Chem. Phys. Lett. **5**, 449–455 (1989)
21. Ramond, T.M., Blanksby, S.J., Kato, S., Bierbaum, V.M., Davico, G.E., Schwartz, R.L., Lineberger, W.C., Ellison, G.B.: Heat of formation of the hydroperoxyl radical HOO via negative ion studies. J. Phys. Chem. A **106**, 9641–9647 (2002)
22. Bartmess, J.E.: Negative Ion Energetics Data. In: NIST Chemistry WebBook, NIST Standard Reference Database Number 69. Linstrom, P.J., Mallard, W.G. (Eds.) National Institute of Standards and Technology, Gaithersburg MD, 20899. Available at: http://webbook.nist.gov. Accessed October 15, 2015
23. Jolly, W.L.: Modern Inorganic Chemistry, 2nd edn. McGraw-Hill, New York (1991)
24. Chiu, F.C.K., Lo, C.M.Y.: Observation of amide anions in solution by electrospray ionization mass spectrometry. J. Am. Soc. Mass Spectrom. **11**, 1061–1064 (2000)
25. Blanksby, S.J., Dua, S., Bowie, J.H.: Unusual cross-ring S_N2 Reactions of $[M - H]^-$ ions of methoxyacetanilides. Rapid Commun. Mass Spectrom. **9**, 177–179 (1995)
26. Blanksby, S.J., Dua, S., Hevko, J.M., Christie, H., Bowie, J.H.: Anionic migration in aromatic systems effected by collisional activation. Unusual fragmentations of deprotonated anilides containing methoxyl and ethoxyl substituents. Eur. Mass Spectrom. **2**, 33–42 (1996)
27. Blanksby, S.J., Dua, S., Christie, H., Bowie, J.H.: Anionic migration reactions in aromatic systems effected by collisional activation. Deprotonated anilides containing methoxycarbonyl substituents. Rapid Commun. Mass Spectrom. **10**, 478–480 (1996)
28. Vogel, A.L.: Textbook of Practical Organic Chemistry, 3rd ed. Longman, London (1989)
29. Jariwala, F.B., Figus, M., Attygalle, A.B.: Ortho effect in electron ionization mass spectrometry of N-acylanilines bearing a proximal halo substituent. J. Am. Soc. Mass Spectrom. **19**, 1114–1118 (2008)
30. Standard Reference Data Program, National Institute of Standards and Technology, Gaithersburg, MD. Standard Reference Database IA. Available at: http://www.nist.gov/srd/nist1a.htm. Accessed August 6, 2015
31. Yang, Z., Attygalle, A.B.: Aliphatic hydrocarbon spectra by helium ionization mass spectrometry (HIMS) on a modified atmospheric–pressure source designed for electrospray ionization. J. Am. Soc. Mass Spectrom. **22**, 1395–1402 (2011)
32. Frisch, M.J., Trucks, G.W., Schlegel, H.B., Scuseria, G.E., Robb, M.A., Cheeseman, J.R., Scalmani, G., Barone, V., Mennucci, B., Petersson, G.A., Nakatsuji, H., Caricato, M., Li, X., Hratchian, H.P., Izmaylov, A.F., Bloino, J., Zheng, G., Sonnenberg, J.L., Hada, M., Ehara, M., Toyota, K., Fukuda, R., Hasegawa, J., Ishida, M., Nakajima, T., Honda, Y., Kitao, O., Nakai, H., Vreven, T., Montgomery Jr., J.A., Peralta, J.E., Ogliaro, F., Bearpark, M., Heyd, J.J., Brothers, E., Kudin, K.N., Staroverov, V.N., Keith, T., Kobayashi, R., Normand, J., Raghavachari, K., Rendell, A., Burant, J.C., Iyengar, S.S., Tomasi, J., Cossi, M., Rega, N., Millam, J.M., Klene, M., Knox, J.E., Cross, J.B., Bakken, V., Adamo, C., Jaramillo, J., Gomperts, R., Stratmann, R.E., Yazyev, O., Austin, A.J., Cammi, R., Pomelli, C., Ochterski, J.W., Martin, R.L., Morokuma, K., Zakrzewski, V.G., Voth, G.A., Salvador, P., Dannenberg, J.J., Dapprich, S., Daniels, O., Farkas, A.D., Foresman, J.B., Ortiz, J.V., Cioslowski, J., Fox, D.J.: Gaussian 09, Revision D.01. Gaussian, Inc, Wallingford (2013)
33. Becke, A.D.: Density-functional exchange-energy approximation with correct asymptotic behavior. J. Chem. Phys. **98**, 5648–5652 (1993)
34. Burk, P., Koppel, I.A., Koppel, I., Leito, I., Travnikova, O.: Critical test of performance of B3LYP functional for prediction of gas-phase acidities and basicities. Chem. Phys. Lett. **323**, 482–489 (2000)
35. Galliani, G., Rindone, B.: Aromatic hydroxylation of benzylamides by potassium superoxide. Tetrahedron **37**, 2313–2317 (1981)